Week 2-8

Optical Detectors 3

Morphology
Materials
Active Region Architecture
Transparency

Chapter 7.4

The central importance of morphology

From ideal diode theory

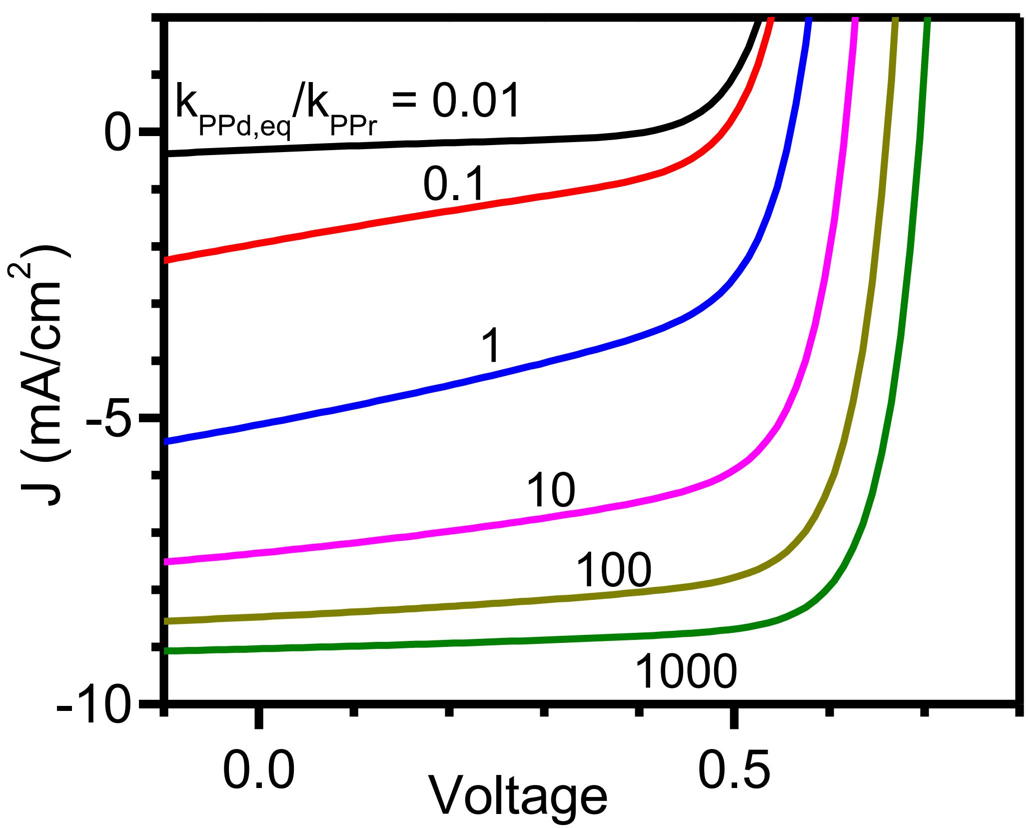

- PP recombination ⇒Reverse Slope
- Best morphologies limit k_{PPr} at interface:
  - **Steric hindrance**
  - **Disorder at interfaces/order in the bulk**

Organic Electronics
Stephen R. Forrest

Morphology Dependence of V_{OC}

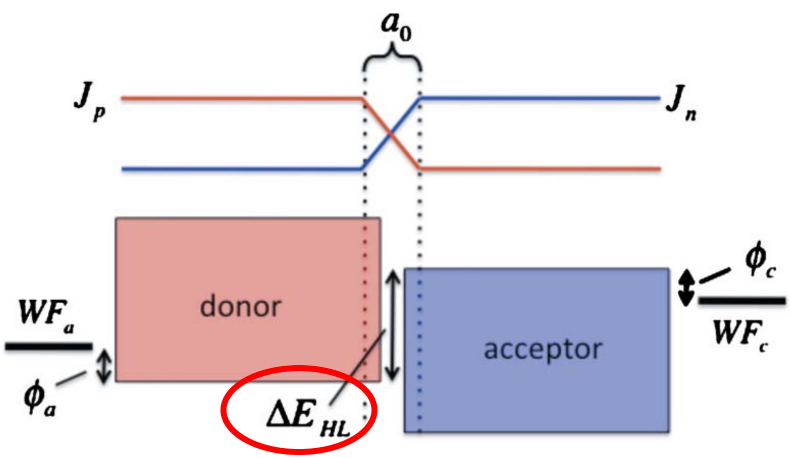

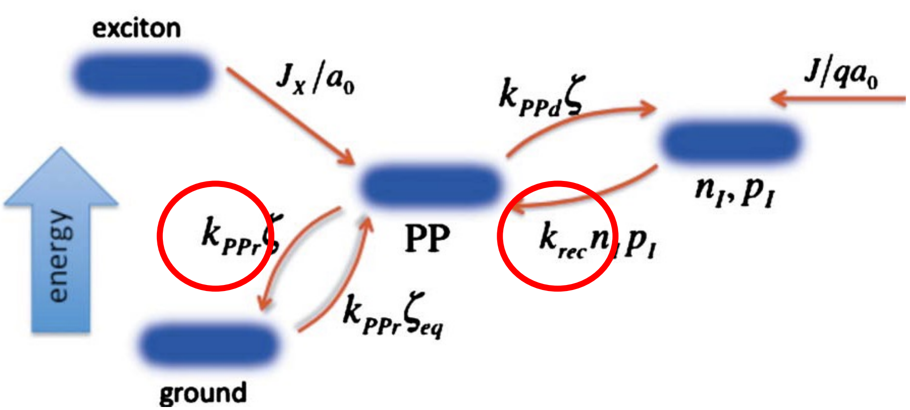

$$qV_{OC} = \Delta E_{HL} - nk_B T \ln\left[\frac{k_{PPr}}{k_{PPd}} \frac{k_{rec} N_L N_H}{J_X / \alpha_0}\right].^*$$

- Material choice determines:
  - ➢ ΔE_{HL} (HOMO-LUMO Gap)
  - ➢ Steric hindrance (MO overlap)
- Device processing/morphology can limit V_{OC} losses:
  - ➢ k_{rec} (PP formation)
  - ➢ k_{PPr} (PP recombination)

*Giebink *et al.* Phys. Rev. B 82 155305 2010

Controlling Interface Morphology to Affect Recombination ($\Rightarrow V_{OC}$)

SVA of Squaraine/Fullerene Solar Cells (see Ch. 4.7)

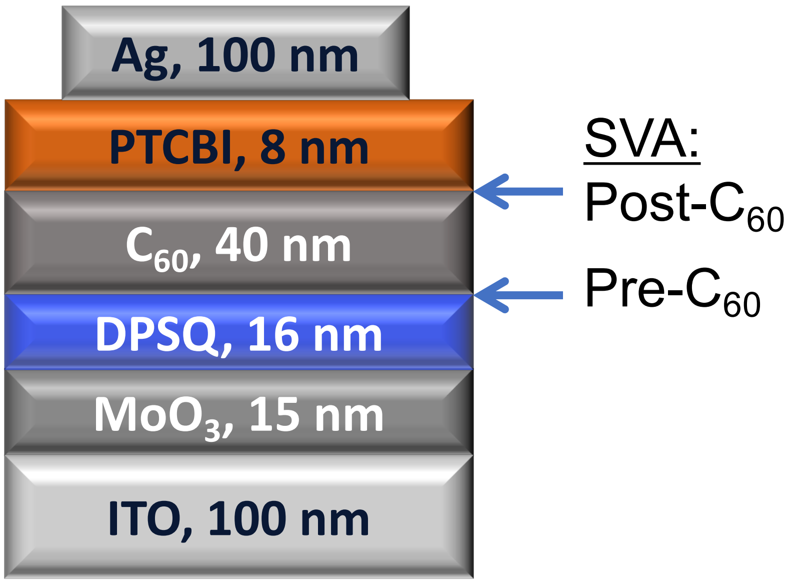

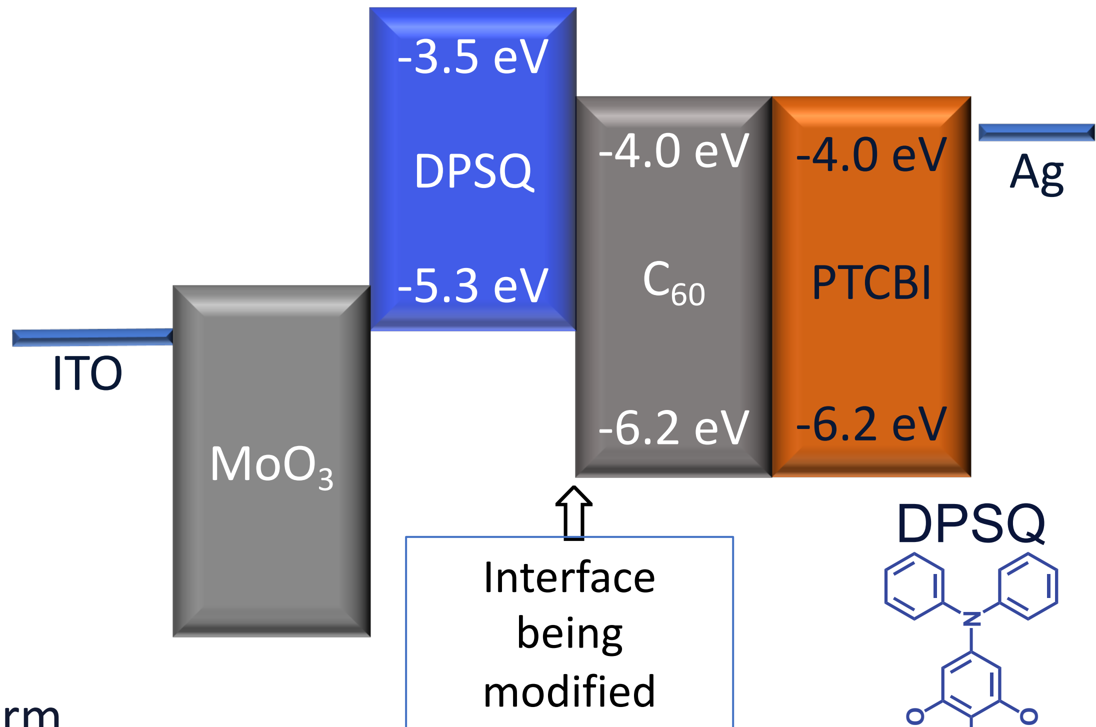

- DPSQ is spun cast from chloroform.
- Other layers deposited by thermal evaporation.
- **Vary D-A interface order via solvent vapor annealing** (SVA):
  - 10 min exposure to dichloromethane vapor to “anneal” squaraine component.

DPSQ

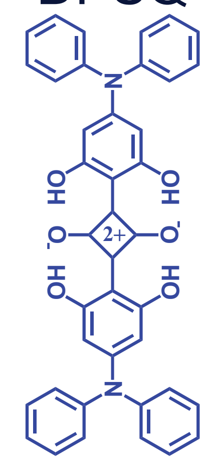

cs
st

SVA Pre-C_{60}

As Cast DPSQ

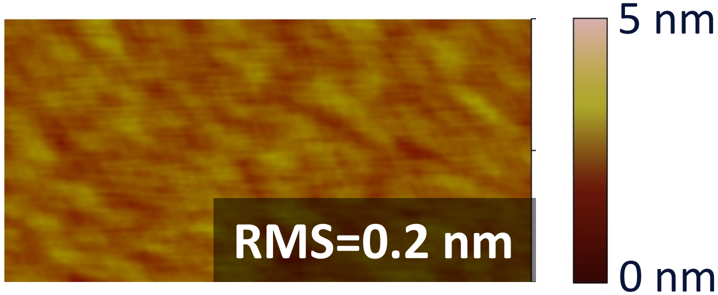

DPSQ SVA pre-C_{60}

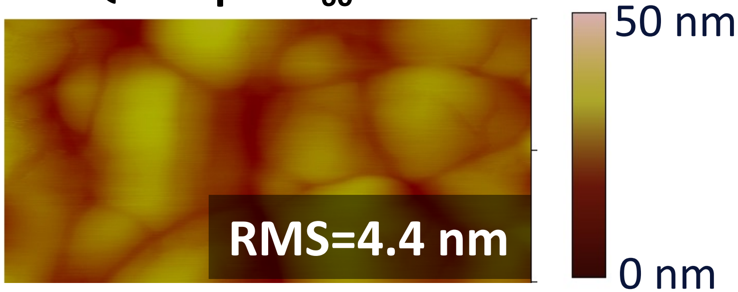

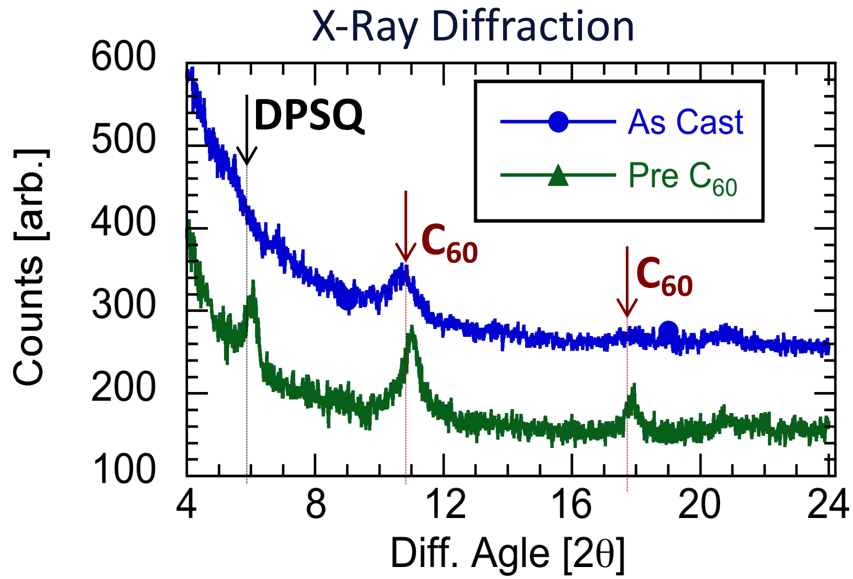

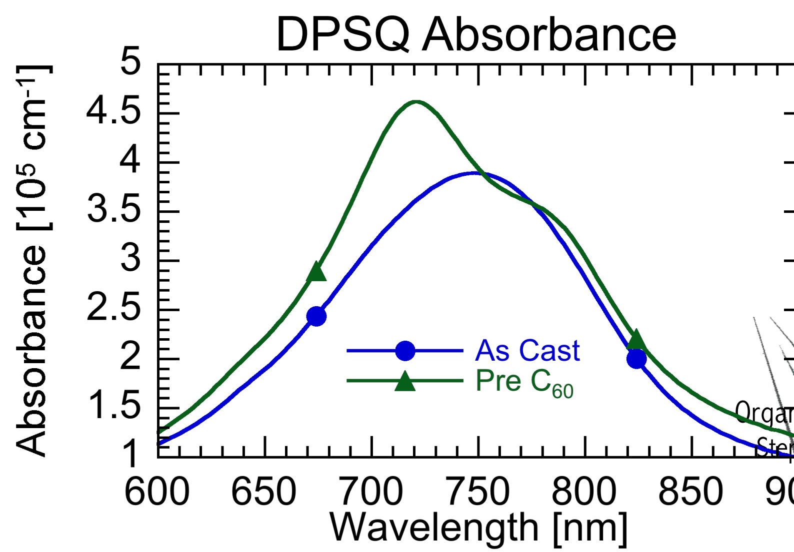

- SVA Pre C_{60}:
  - Crystallizes and roughens DPSQ.
  - Crystalline DPSQ templates *quasi-epitaxial* C_{60} growth.

Devices with SVA Post-C_{60}

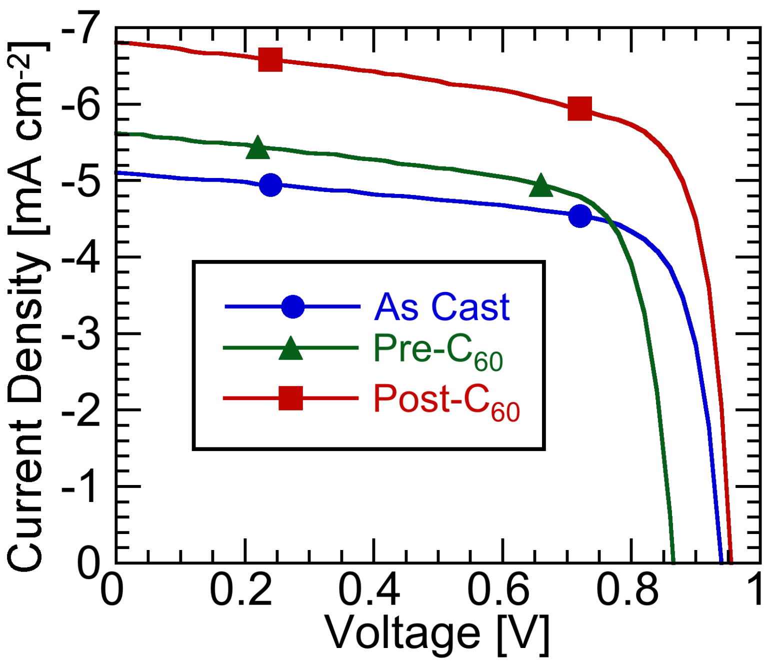

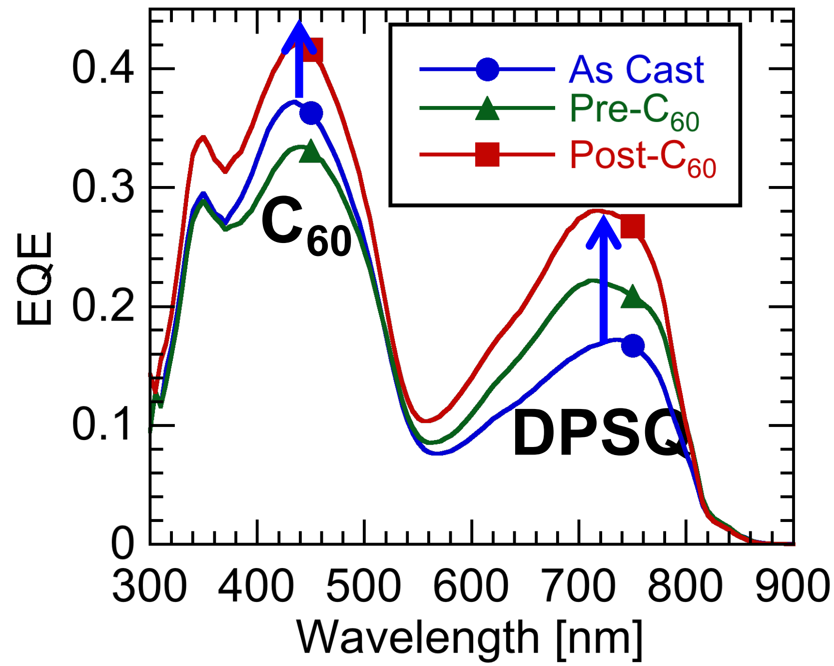

- SVA post-C_{60}
  - DPSQ EQE ⇑ 80%.
  - J_{SC} ⇑ 25%.
- No loss in V_{OC}
  - k_{PPr} unchanged.

Process	J_{SC}[mA cm^{-2}]	V_{OC} [V]	FF [%]	η_P [%]
As Cast	5.3±0.3	0.94	73	3.6±0.2
Pre-C_{60}	5.6±0.3	0.86	70	3.4±0.2
Post-C_{60}	7.0±0.4	0.96	71	4.8±0.3

J. D. Zimmerman, et al. Nano Lett. 12, 4366 (2012)

anic Electronics
ephen R. Forrest

Achieving the Ideal Interface Morphology

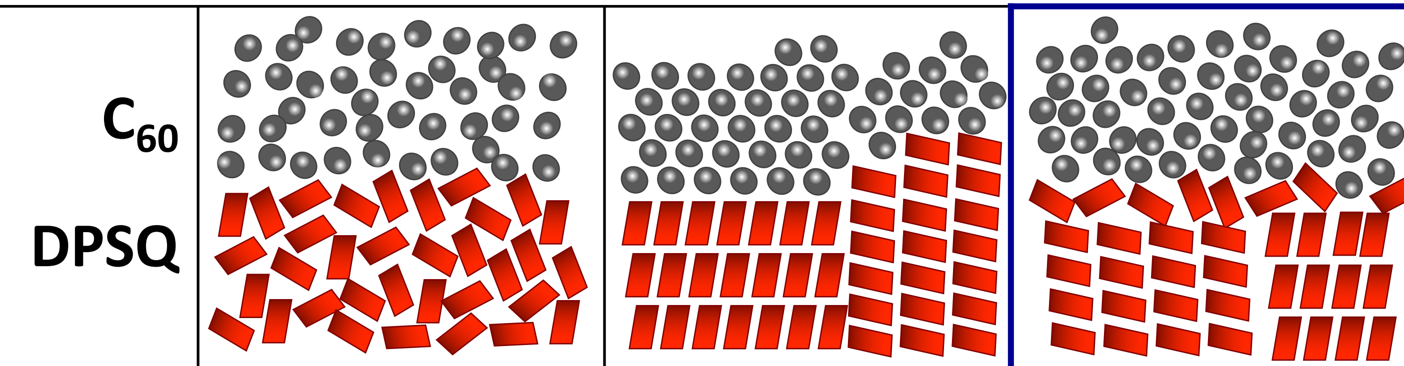

	As Cast	Pre C_{60}	Post C_{60}
Bulk DPSQ	Amorphous	Ordered	Mod. Order
Bulk C_{60}	Weak order	Ordered	Weak Order
Interface	Disordered	Ordered	Disordered
Surface	Smooth	Rough	Smooth
k_{PPr}	Low	High	Low
V_{OC}	High	Low	High
J_{SC}	Low	Moderate	High

J. D. Zimmerman, et al. Nano Lett. (2012)

Morphology vs. V_{OC}

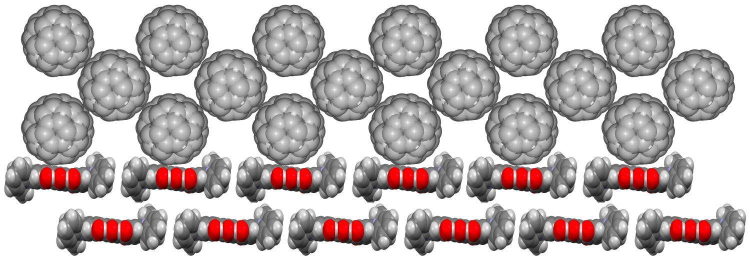

$$qV_{OC} = \Delta E_{HL} - nk_B T \ln\left[\frac{k_{PPr}}{k_{PPd}} \frac{k_{rec} N_L N_H}{J_X / \alpha_0}\right]$$

$$k_{rec} = \gamma = \frac{q}{\varepsilon}\left(\mu_e + \mu_h\right)$$

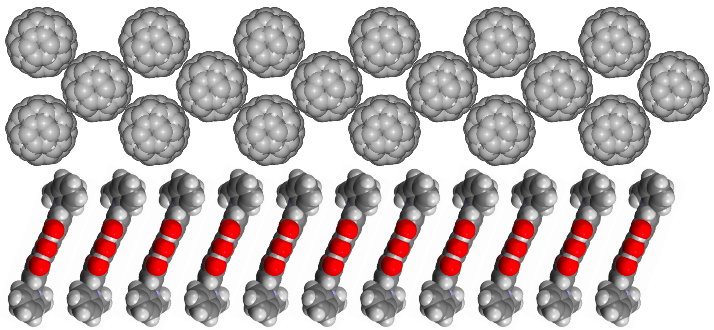

- Worst case scenario: perfectly ordered crystalline interface and bulk, Face-on .
  - High k_{PPr} and k_{rec}

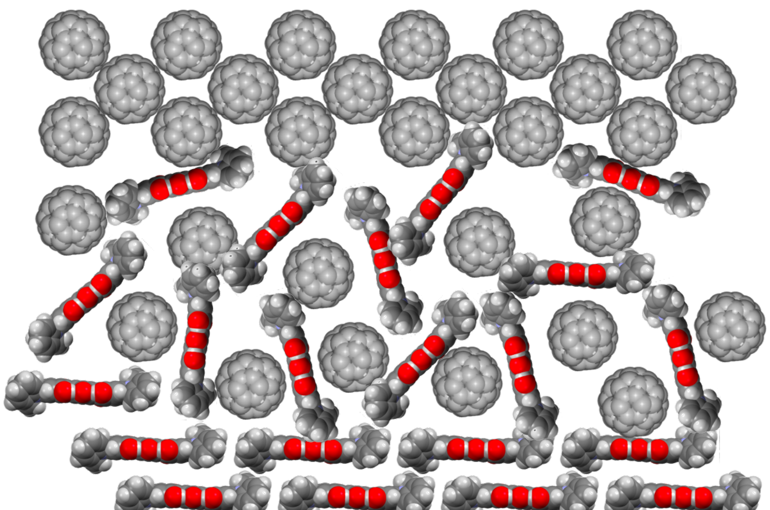

- Better Scenario I: Perfectly crystalline and end-on orientation

- Even Better Scenario II: crystalline bulk, intermixed interface
  - Poor coupling between like-molecules (C_{60}-C_{60} and SQ-SQ) reduces PP formation (k_{rec}) probability.
  - Overcomes enhanced k_{PPr} due to facial contact

Disorder Dependent CT State Energy at Polymer Junctions

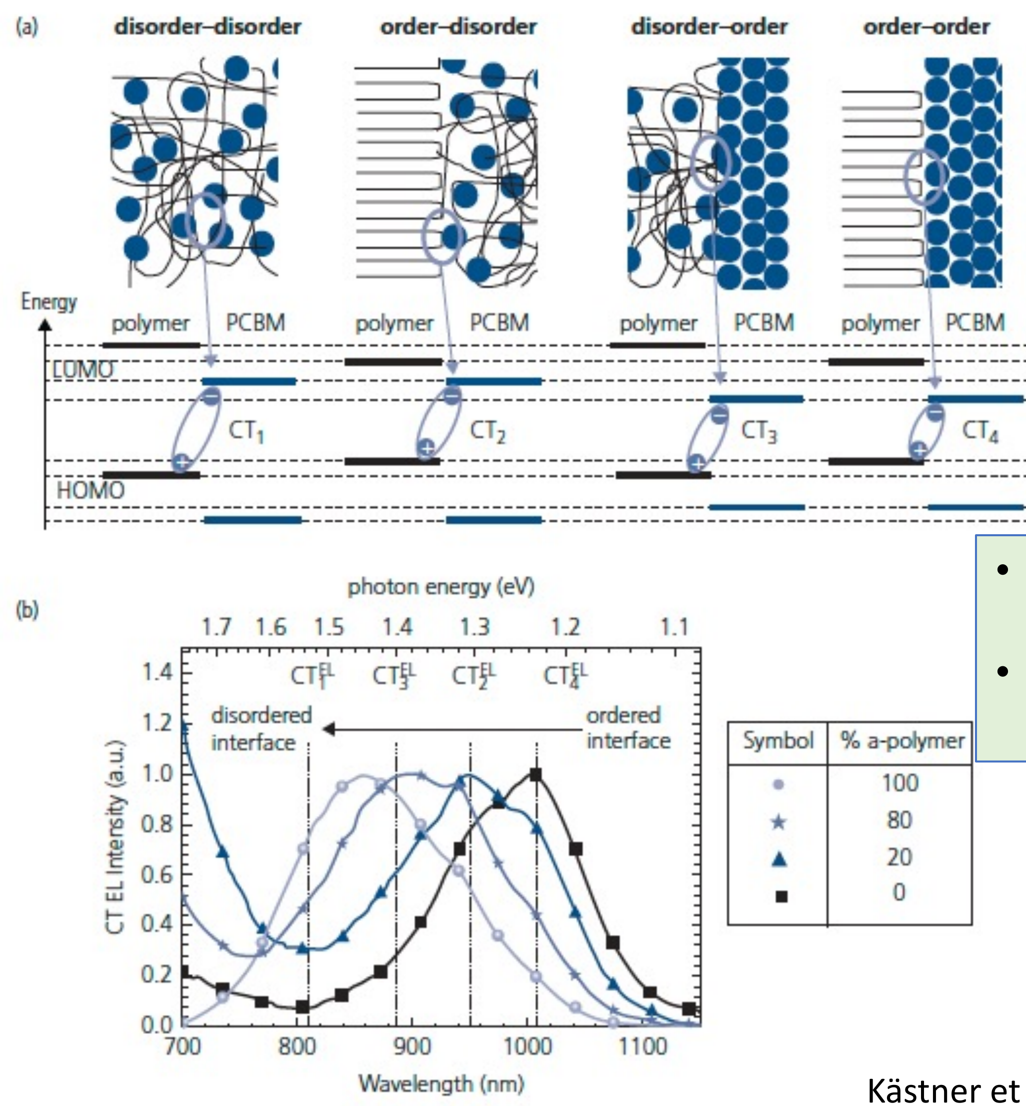

- Morphology at functionalized PPV:PCBM HJs controlled by functionalization and blends
- Qualitatively similar phenomena asfor small molecule (DPSQ:C60) junctions

Kästner et al., Adv. Sci. 4, 1600331 (2017)

Morphology Controls CT State Energy

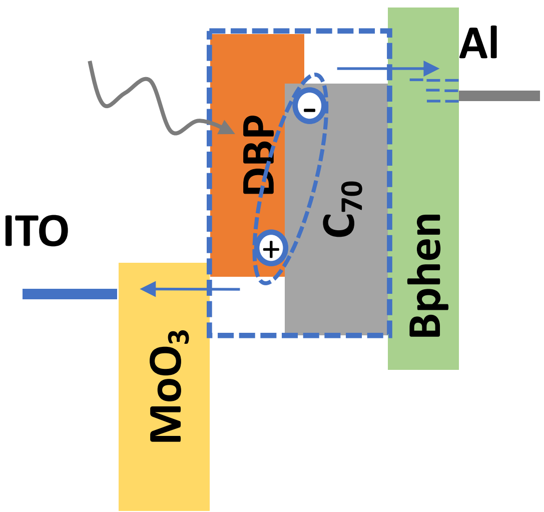

CT states are directly excited optically, or by injection from contacts (operating the OPV in the OLED mode).

Different blend under 3 V bias

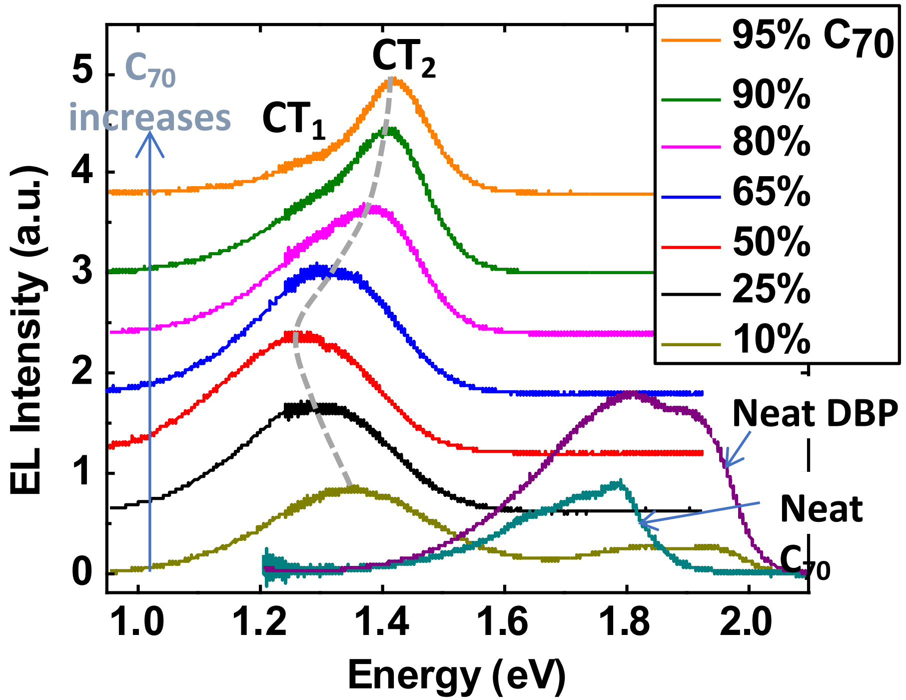

Shift in energy of CT_2 due to morphology changes as the amount of C70 in DBP changes

X. Liu, et al., ACS Nano 10, 7619 (2016).

CT Energy Increases with C_{70} Domain Size⇒ Exciton Confinement

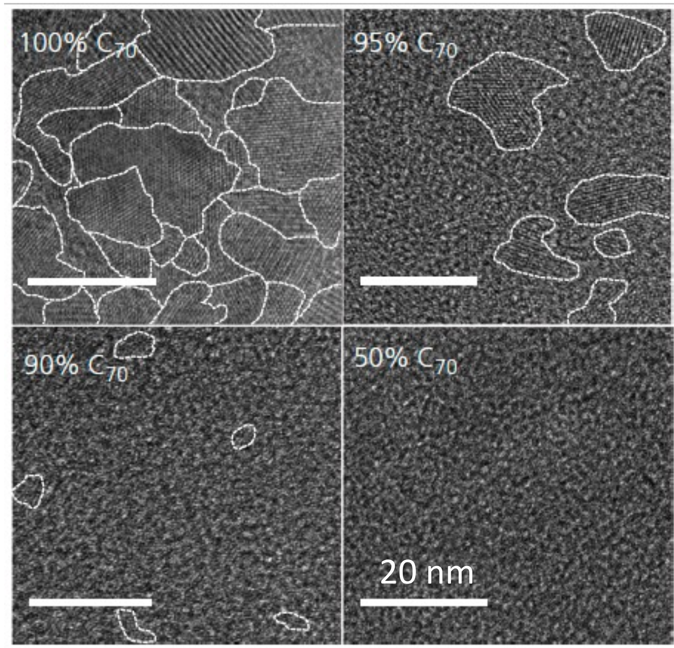

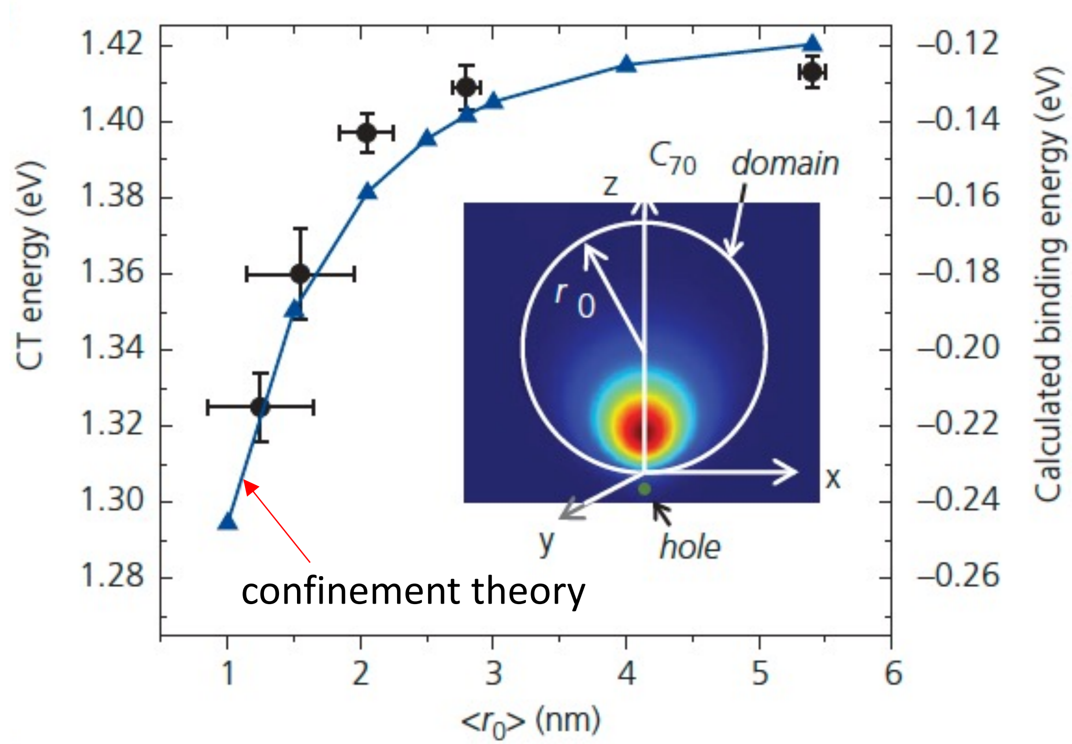

$$H = -\frac{\hbar}{2m_e^*}\nabla^2 + V(\mathbf{r}),$$

$$V(\mathbf{r}) = \begin{cases} -\dfrac{q^2}{4\pi\varepsilon_0\varepsilon_{r,C_{70}}|\mathbf{r}-\mathbf{a}|} & (|\mathbf{r}-\mathbf{r_0}| < r_0) \\ -\dfrac{q^2}{4\pi\varepsilon_0\varepsilon_{r,DBP}|\mathbf{r}-\mathbf{a}|} + \phi_b & (|\mathbf{r}-\mathbf{r_0}| > r_0) \end{cases}$$

- Electron confined to C_{70} domain, hole immobilized on DBP
- Barrier (ϕ_b) exists at C_{70} domain peiphery

X. Liu, et al., ACS Nano 10, 7619 (2016).

New Architectures for Increased Spectral Coverage

Exciton Cascades

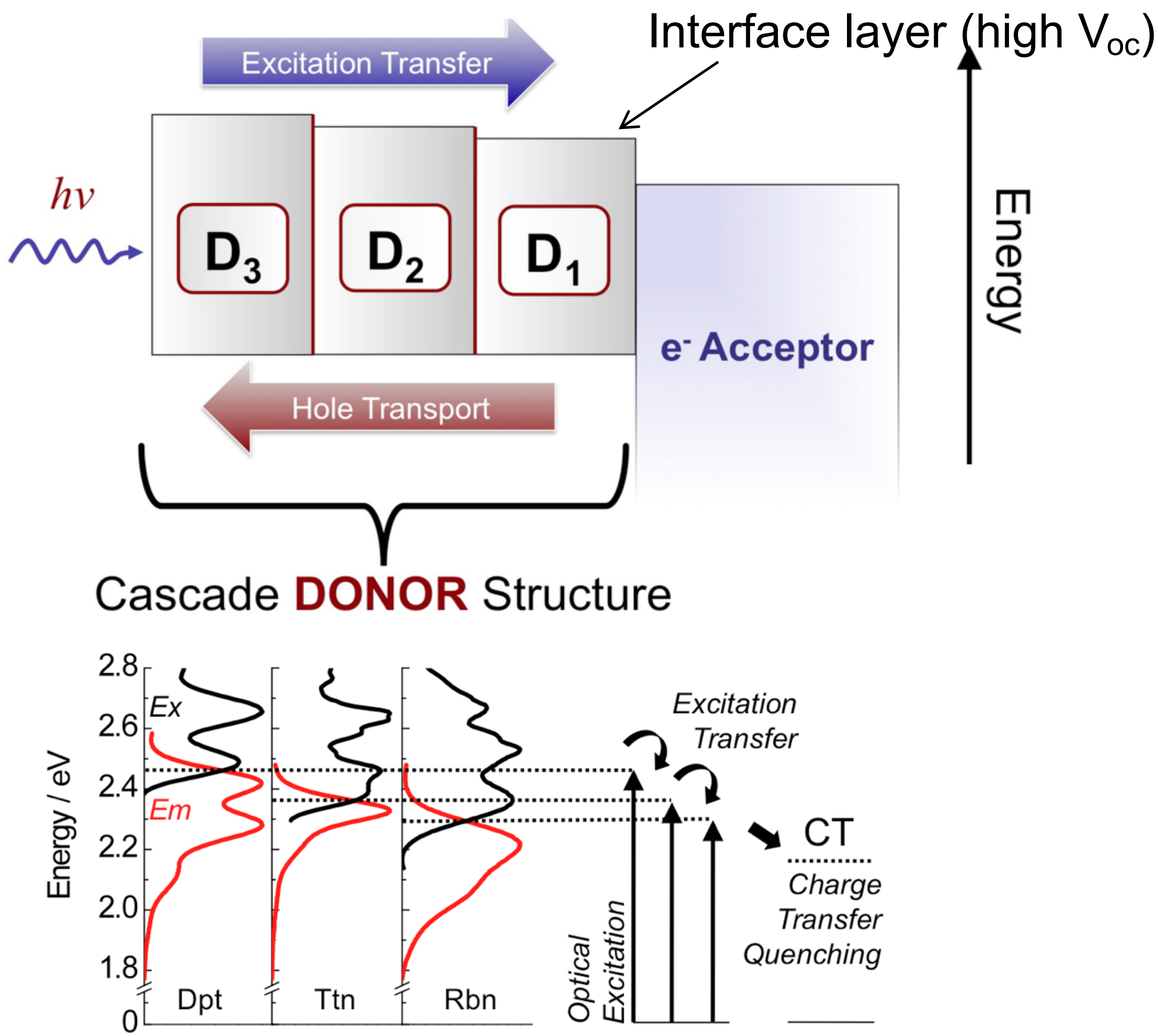

Schlenker, et al., *Chem. Mater.*, **23**, 4132 (2011).

Organic Electronics
Stephen R. Forrest

High Efficiency Donor Cascade Device

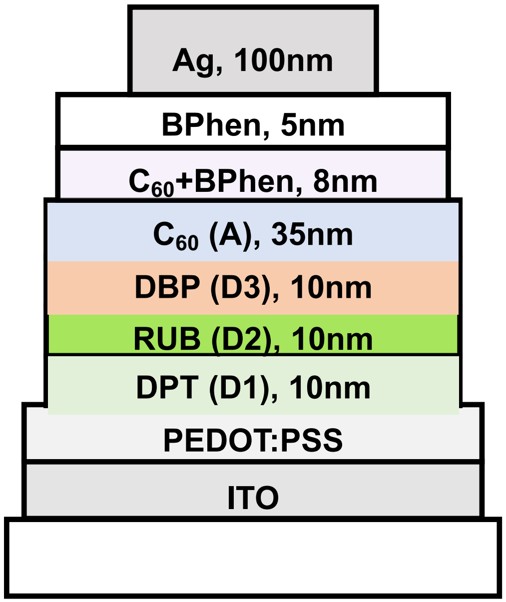

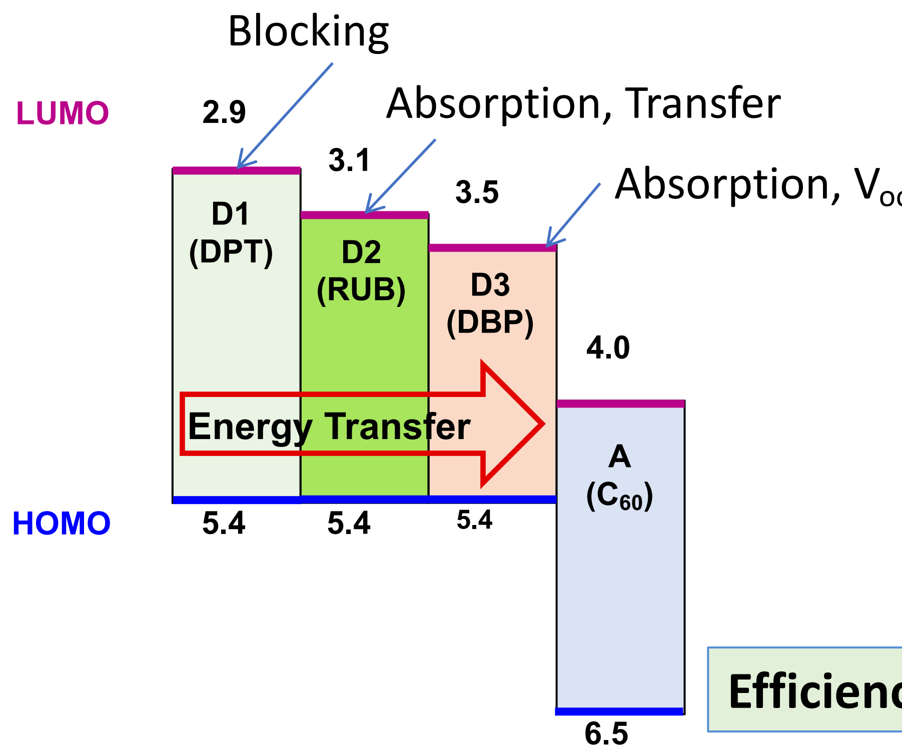

Efficiency: 7.1%

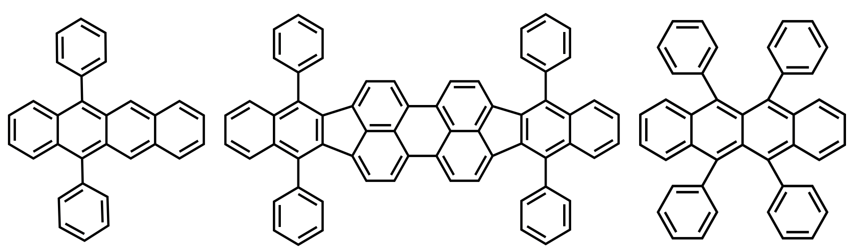

DPT DBP RUB

O. L. Griffith & S. R. Forrest, *Nano Letters*, 14, 2353 (2014).

Ternary BHJs Increase Solar Coverage

Charge Xfer

Energy Xfer

Parallel Junctions

"Alloy" formation

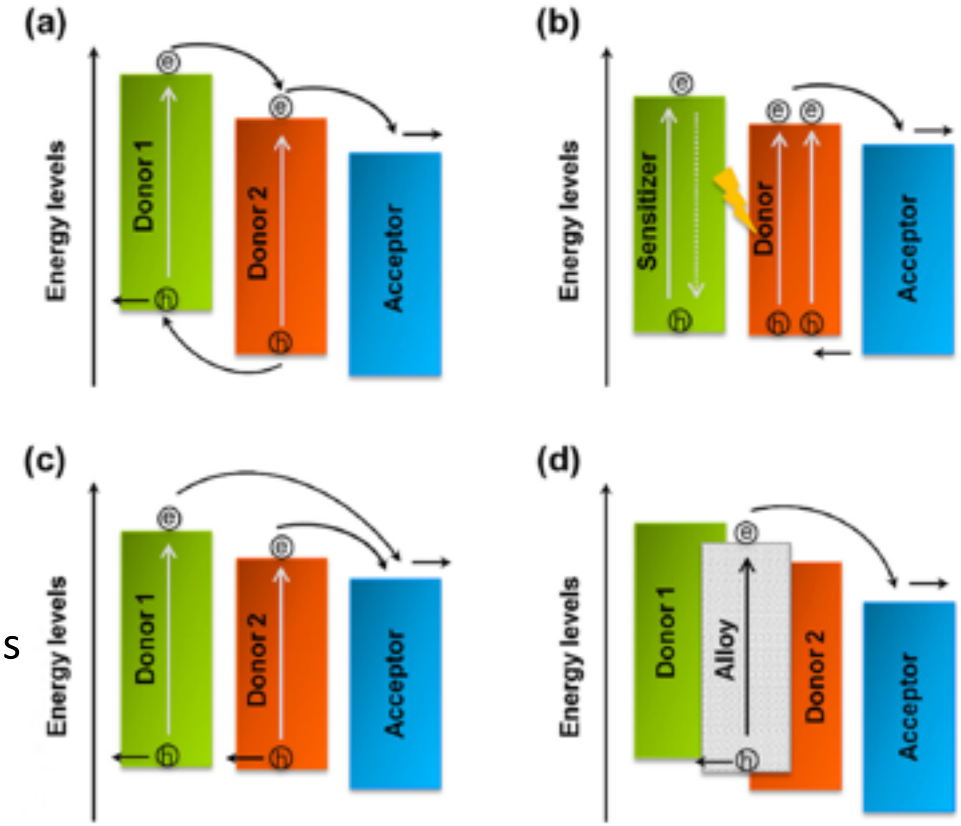

Features of ternary blends:

- V_{OC} of the ternary lies between the extremes of the two subcell junctions
- Materials chosen to cover solar spectrum
- Can be DA_1A_2 or AD_1D_2 junctions
- Morphology is key
- Probably more than one process governs performance
- Molecular alloy formation unlikely

Parallel Junction Ternary OPVs

- V_{OC} intermediate between individual binary OPVs

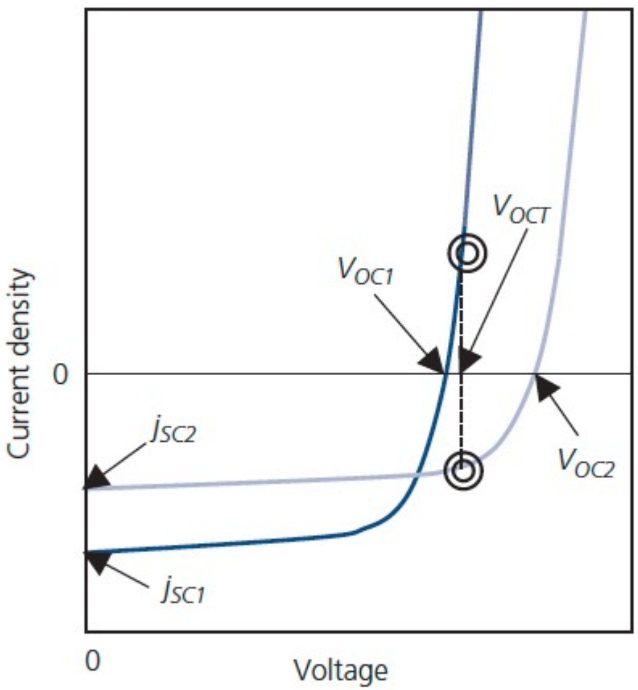

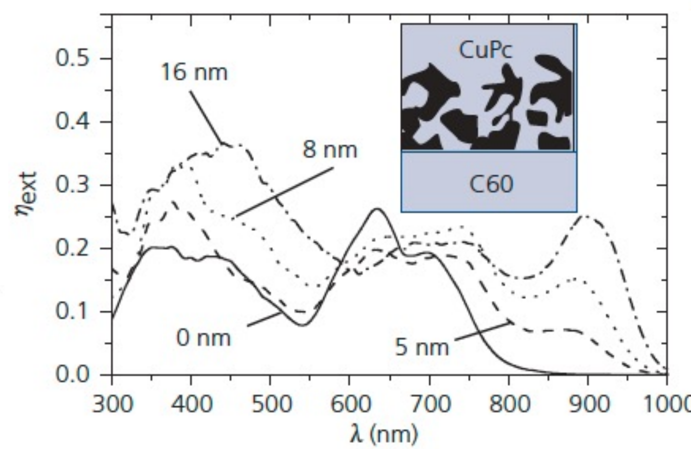

Increased spectral coverage

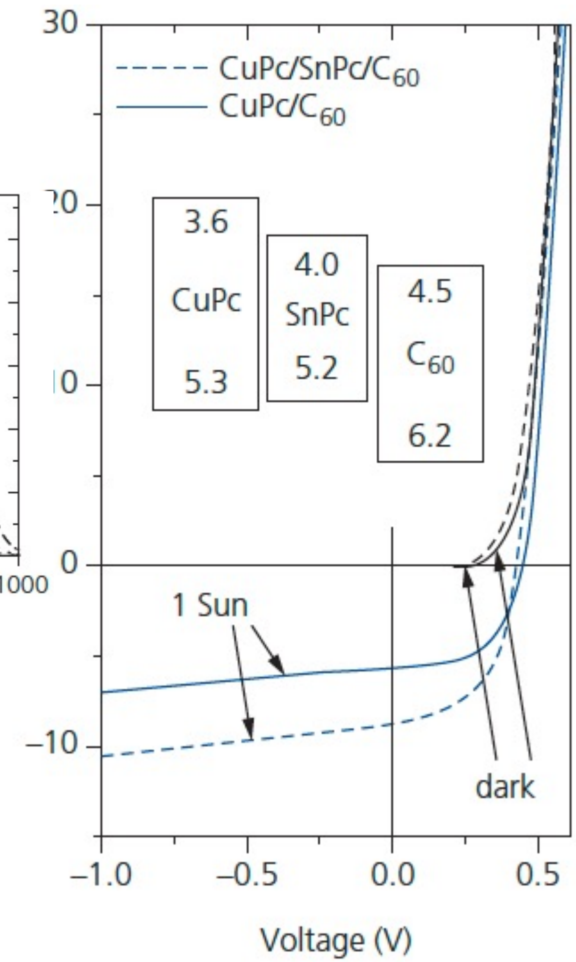

Yang, et al., Appl. Phys. Lett. 92, 38 (2008)

Increased efficiency

Example DA_1A_2 ternary BHJ

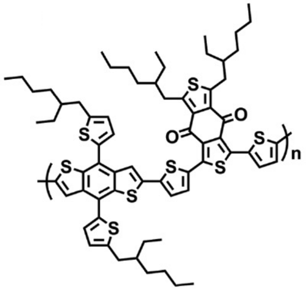

PBDB-T

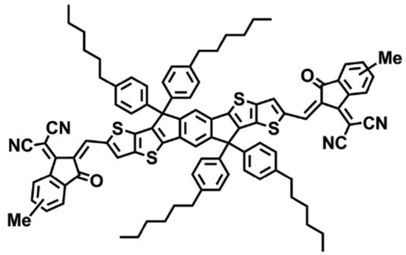

IT-M

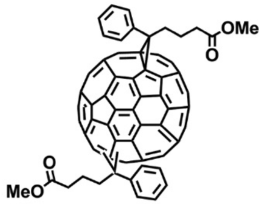

$BisPC_{71}BM$

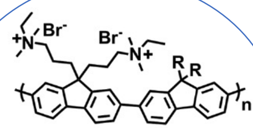

$R=C_8H_{17}$

PFN-Br

Exciton blocker

$D:A_1:A_2$ ratio	V_{OC} (V)	j_{SC}[(a)] (mA/cm^2)	FF	η_P (max) (%)	η_P (ave)[(b)] (%)
1:1:0	0.937	16.7	0.69	10.80	10.45
1:1:0.2	0.952	17.4	0.74	12.20	11.75
1:0:1	1.02	10.6	0.58	6.25	5.86

- Cell area = 4 mm^2.
- Sample size = 100 diodes

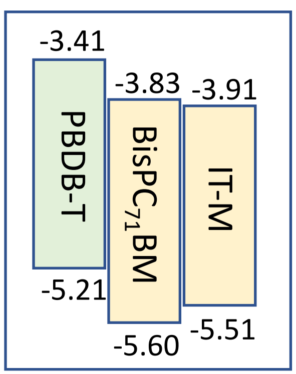

W. Zhao, et al., *Advanced Materials,* **29**, 2, 2017.

Solution-Processed Bi-ternary OPV

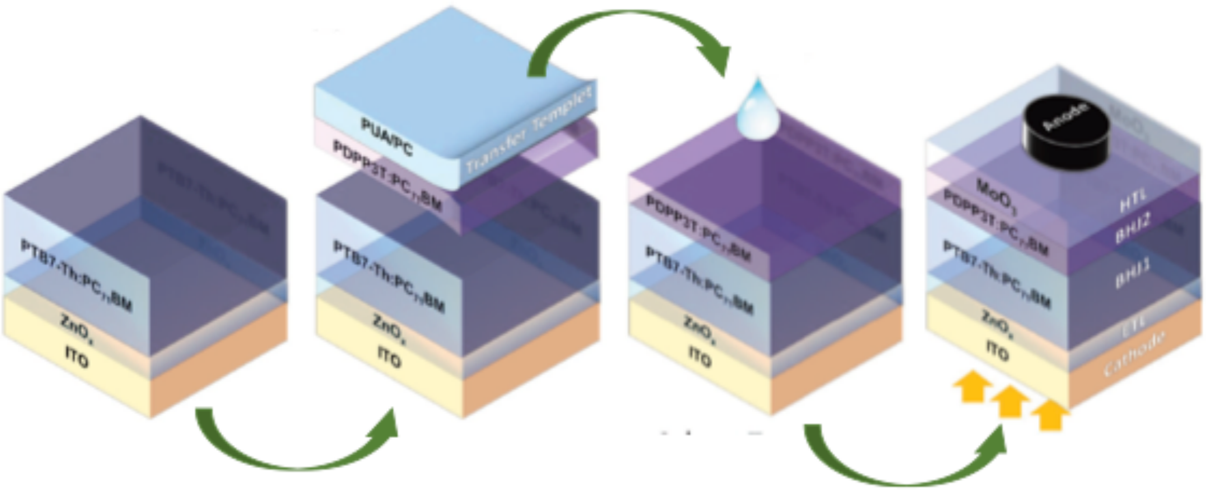

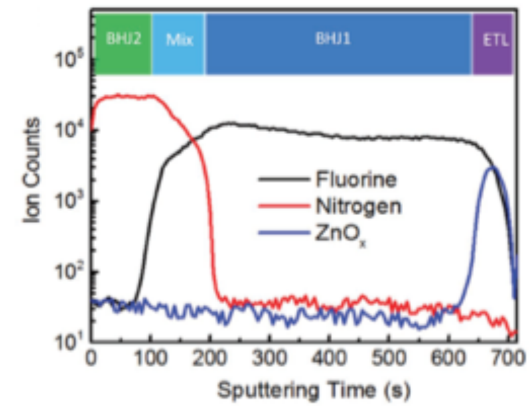

Intermixing of two donors creates continuous hole and electron conduction

Cell[a]	V_{OC} (V)	j_{SC}[b] (mA/cm^2)	FF	η_P (max) (%)	η_P (ave)[c] (%)
BHJ1	0.81	18.5	0.70	10.5	10.3
BHJ2	0.69	7.4	0.71	3.6	3.5
BHJ1/2	0.77	23.8	0.67	12.3	11.9

(b)

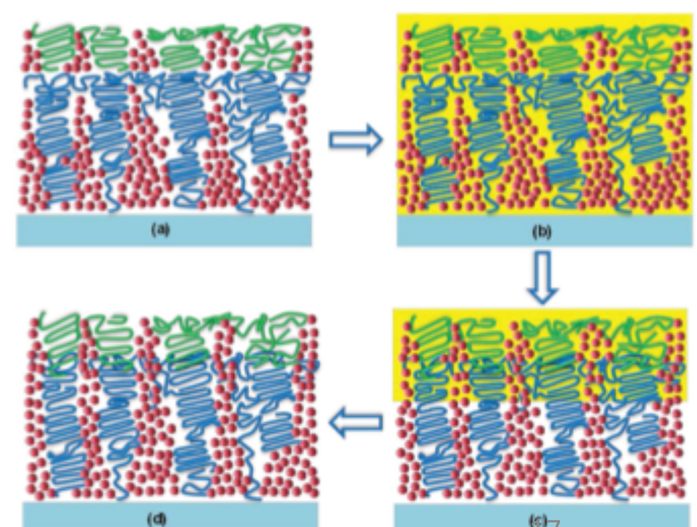

J. Huang, *Advanced Materials,* **29**, 1606729, 2017.

:s
st

Series Connecting Two BHJs: Bi-Ternary OPVs

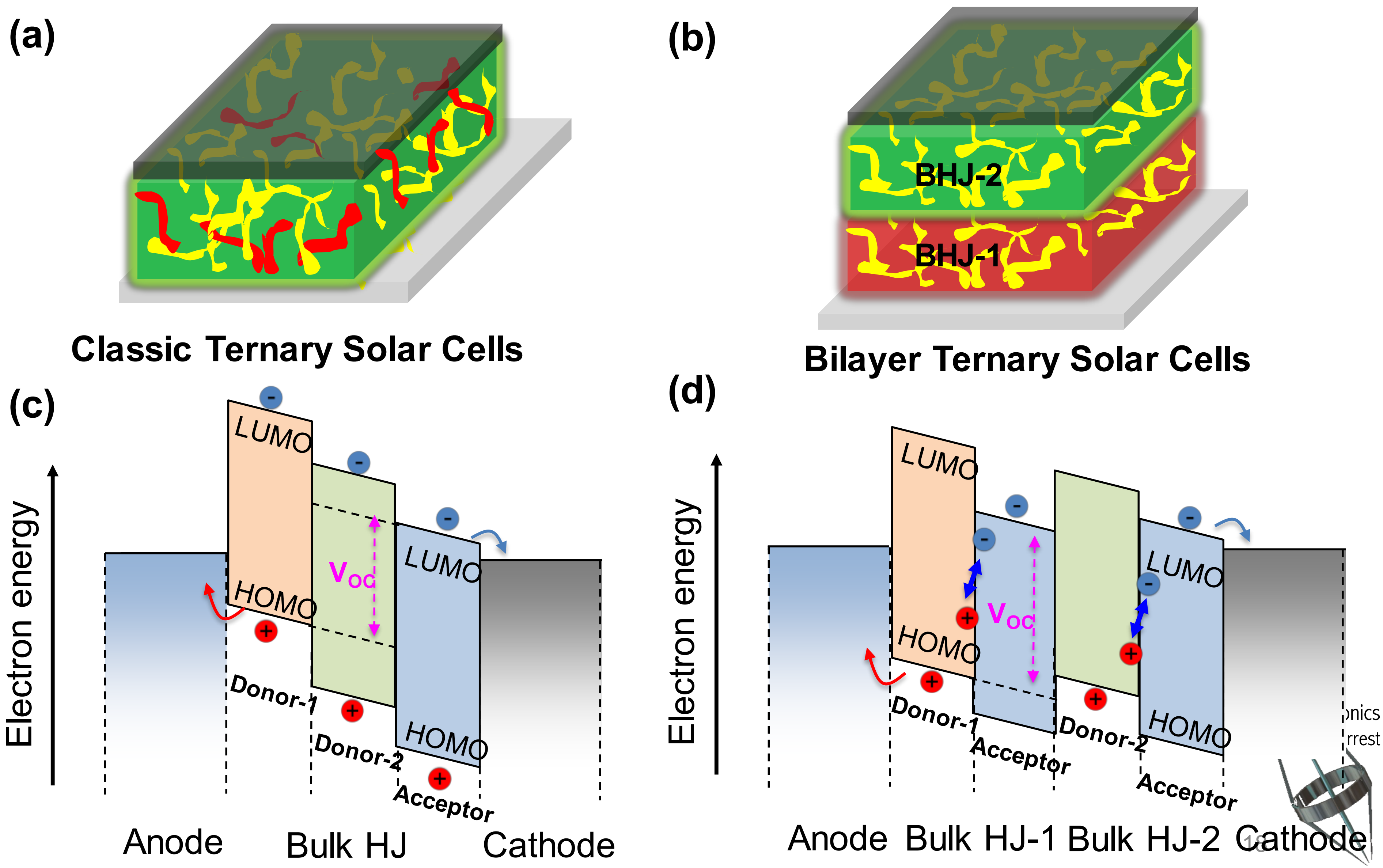

Vacuum Deposited Dipolar Small Molecules in Biternary OPVs

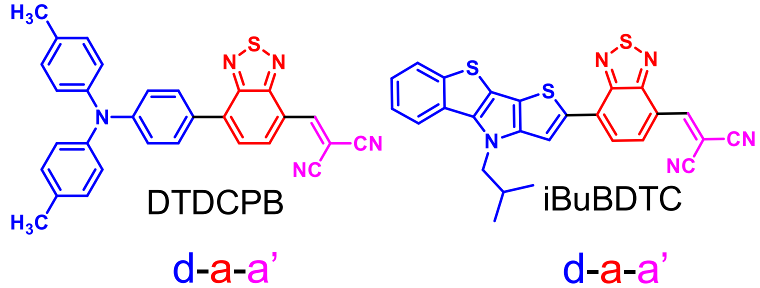

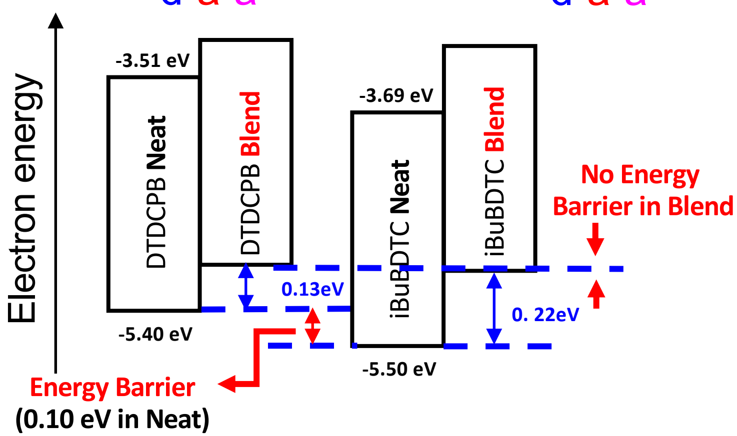

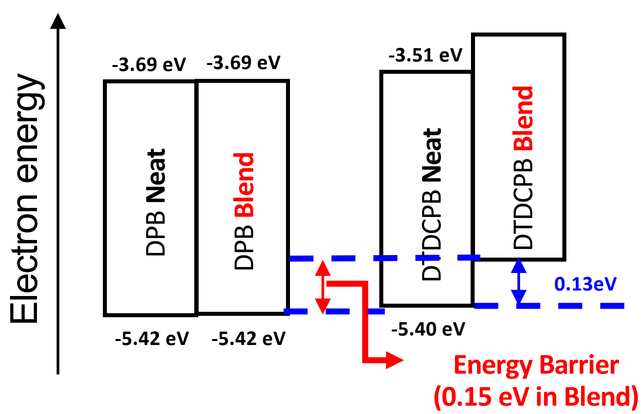

- Large dipole moment of d-a-a' donors evens the HOMO energies of the two when blended, allowing for continuous pathways for holes.
- Electrons conducted by common C_{70} acceptor

Device	j_{SC} [mA/cm^2]	V_{OC} [V]	FF [%]	η_P [%]
Binary (BTDC-Fo, 80 nm)	14.8	0.98	57.7	8.5
Binary (DTDCPB, 80 nm)	15.0	0.89	68.5	9.2
Bi-ternary (60 nm)	13.7	0.98	70.0	9.4

Li, et al. J. Am. Chem. Soc. 121, 18204 (2018)

Designing Materials for OPVs

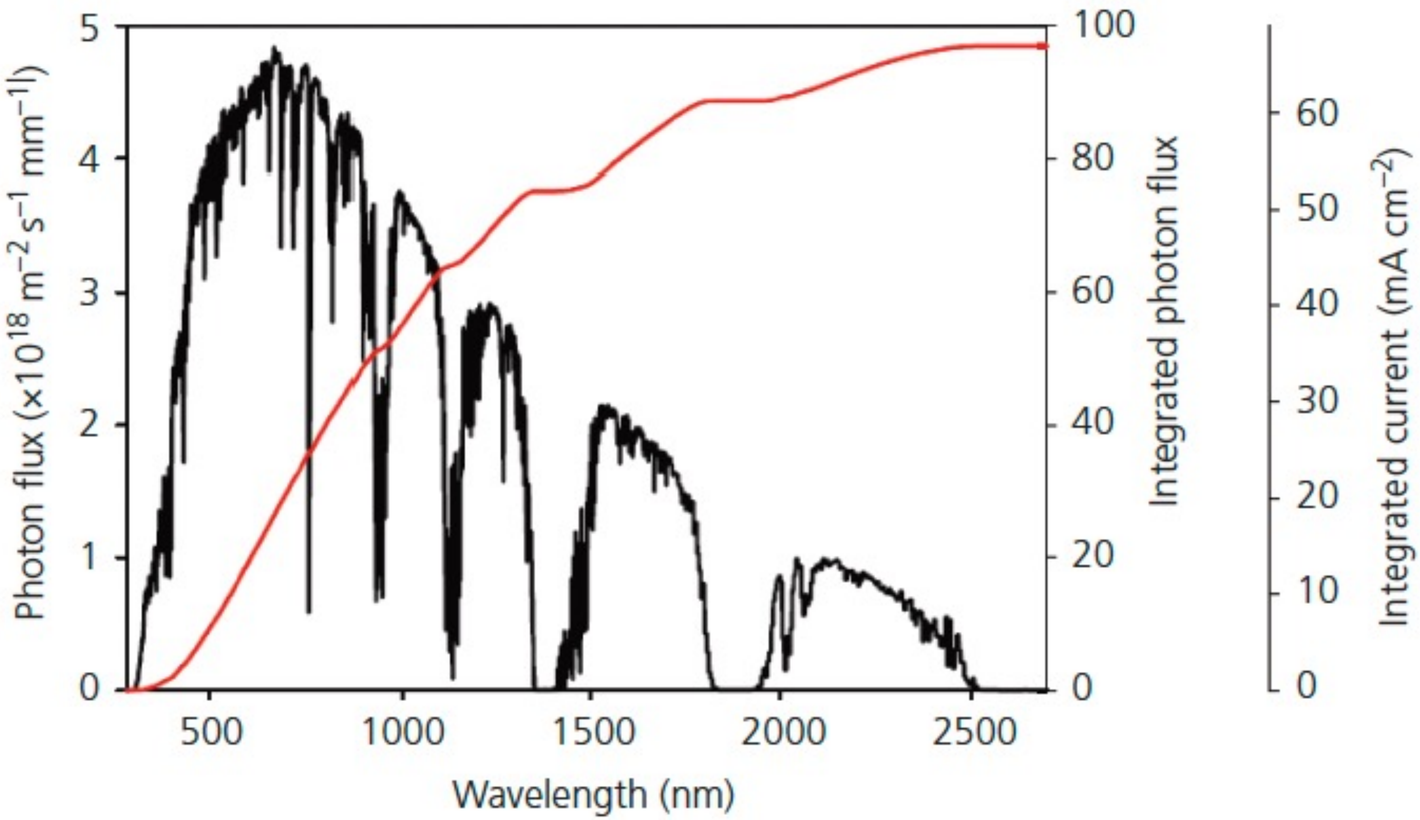

- Most of the usable (by single junction cell) spectrum is at λ < 1.5 µm
- Thermodynamic limits are reached at λ ~ 1 µm
- These considerations guide materials choices

Modular design of materials

- A method of functionalizing molecular cores to :
  - ➢ tailor wavelength coverage
  - ➢ improve morphology to achieve crystalline of appropriate scale
  - ➢ increase charge mobility
- Example: donor architecture

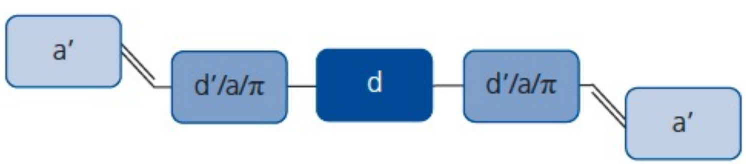

a=electron withdrawing (acceptor-like) moiety
d=electron donating (donor-like) moiety
π=bridge group

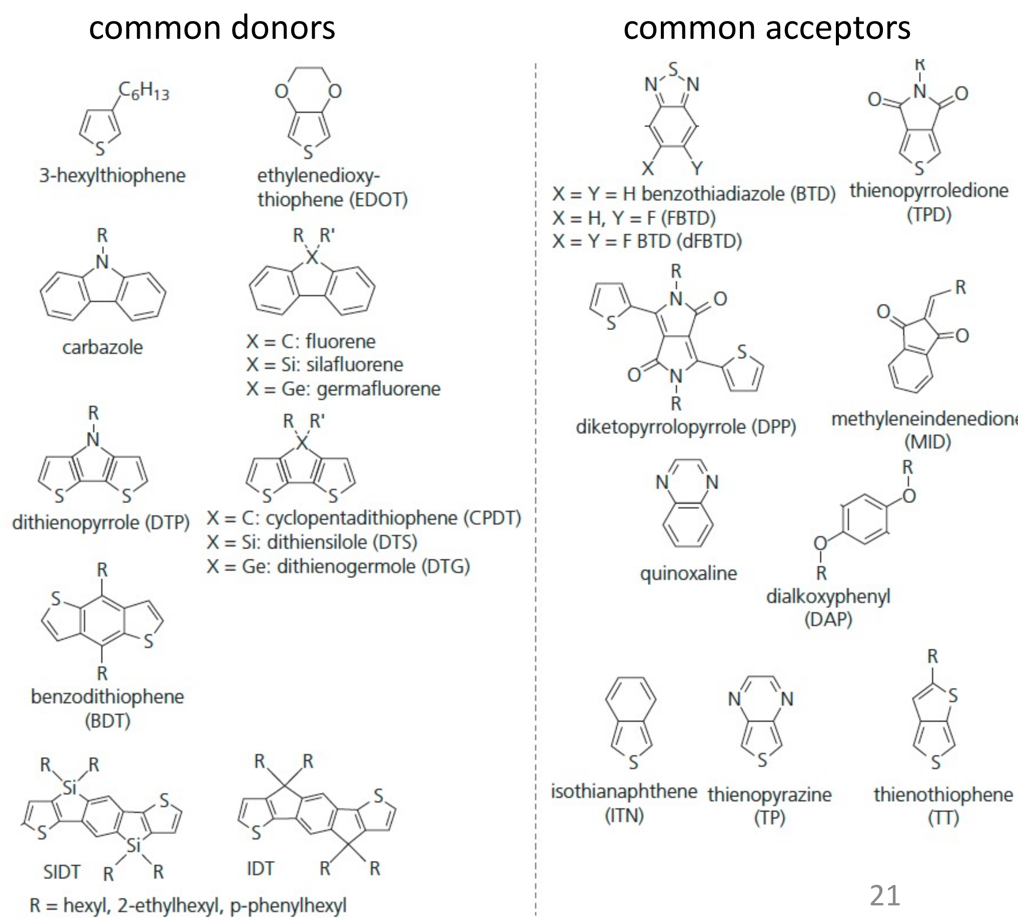

Squaraine Donors: Functionalized to improve stacking

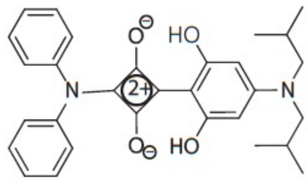

ASSQ

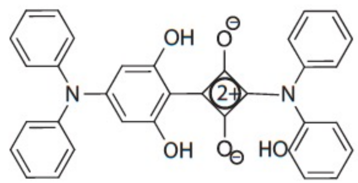

DPASQ

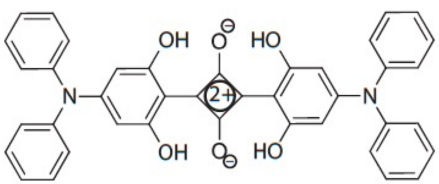

DPSQ

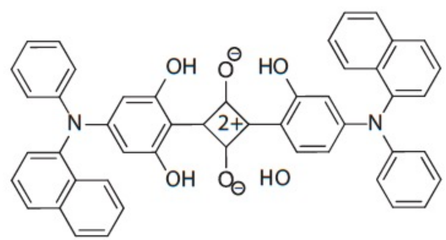

1-NPSQ

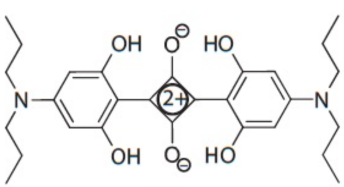

PSQ

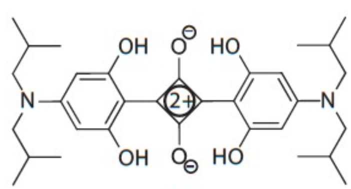

SQ

parent molecule

Phenyl groups promote planar π-stacking
⇒increased hole mobility
⇒increased fill factor

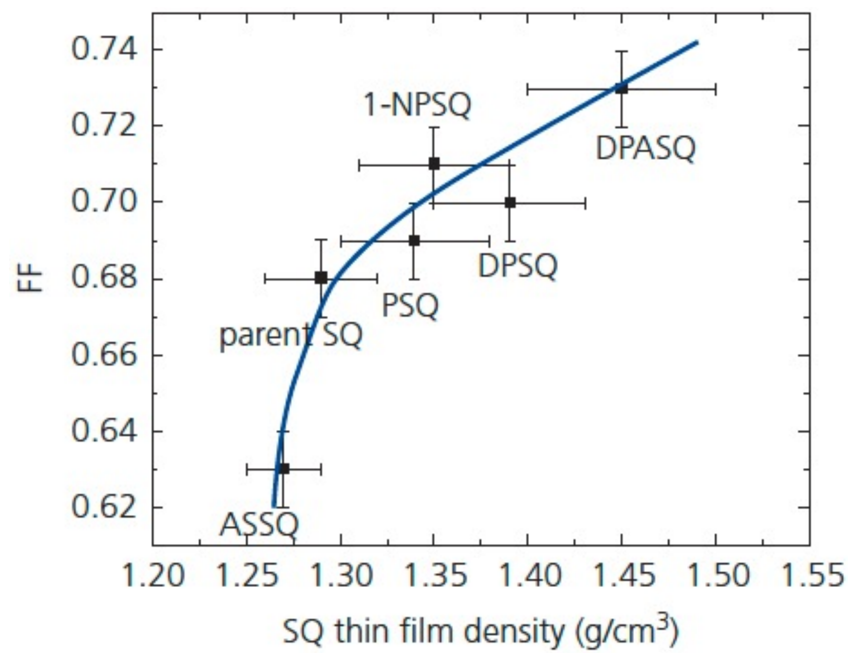

Wei et al., ACS Nano 6, 972 (2011)

Oligothiophenes: Extending the core to increase the conjugation length

- Longer electron conjugation ⇒ lower excited state energy ⇒red shift in absorption

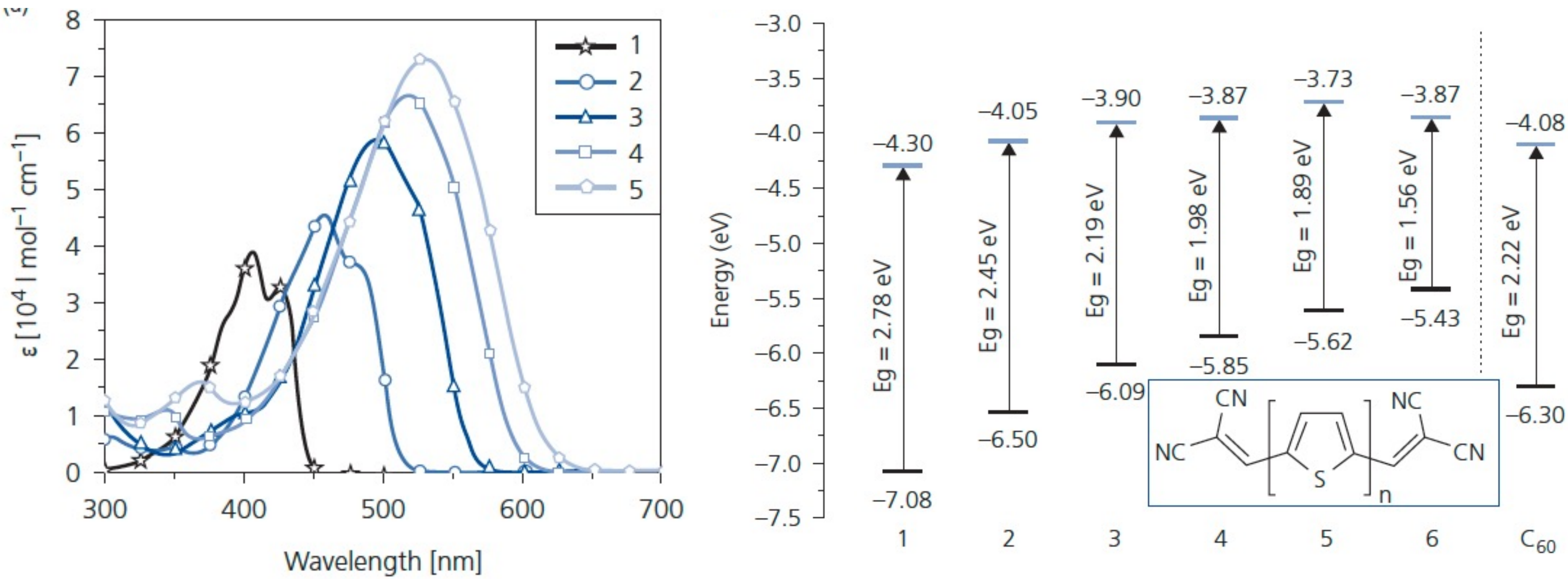

Fitzner et al., Adv. Functional Mater. 21, 897 (2011)

Non-Fullerene Acceptors

Molecules perfectly adapted for wavelength coverage and high conductivity

- Thiophene donor cores extended for increased conjugation
- Cores protected by alkane groups that also enhance solubility
- Acceptor end groups unprotected to enhance π-stacking

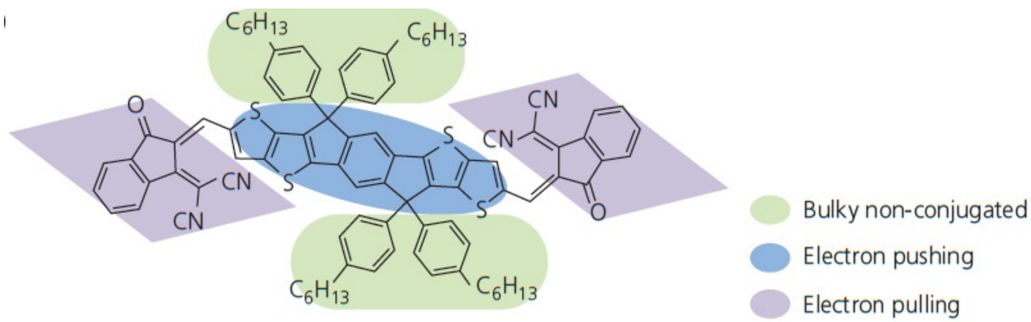

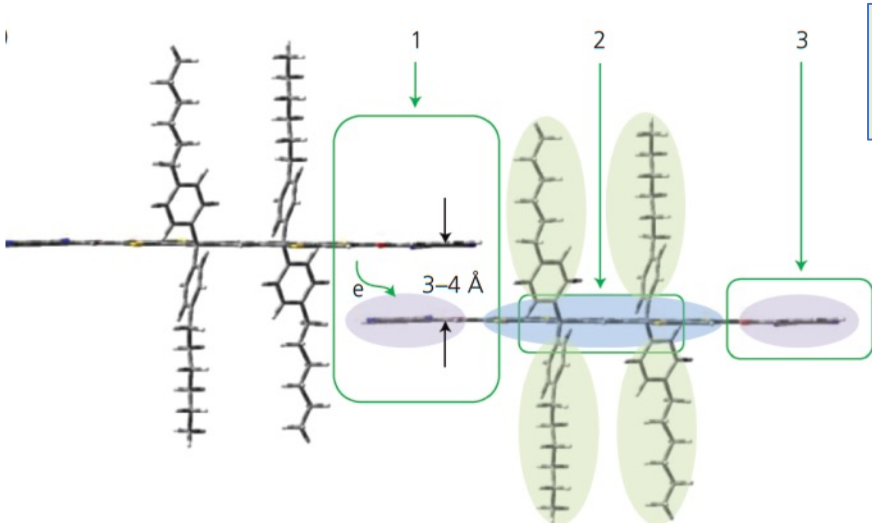

Architecture of thiophene-based NFAs has several common elements

Hou et al., Nat. Mater., 17, 119 (2018)

Non Fullerene Acceptor Design To Selectively Absorb Into the NIR

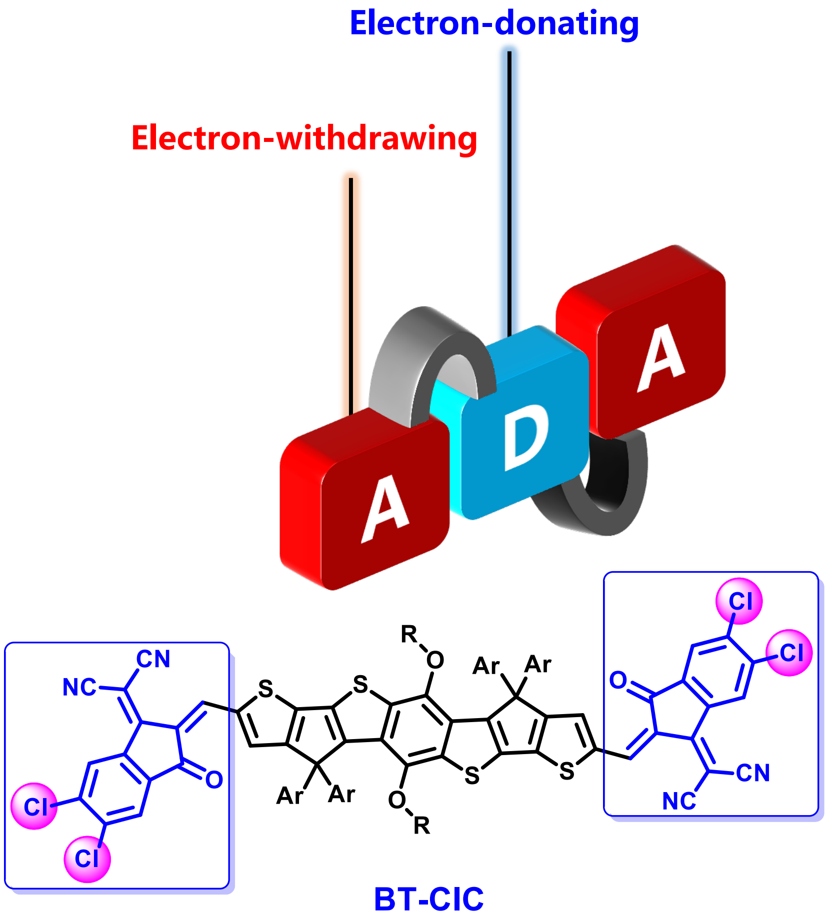

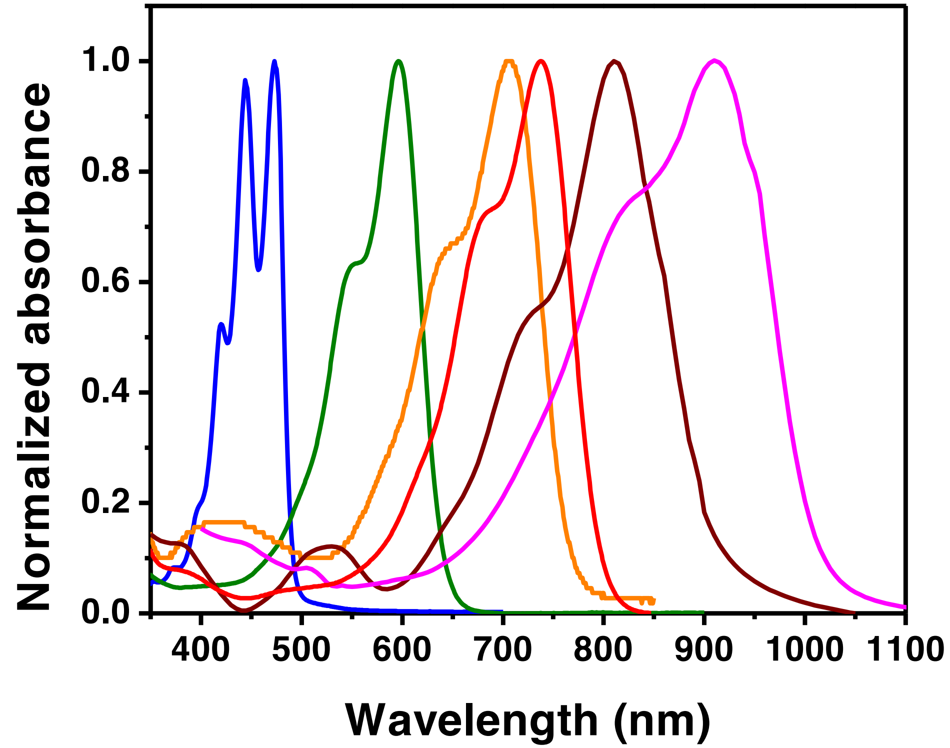

Absorption tunability presents opportunities unique to OPVs

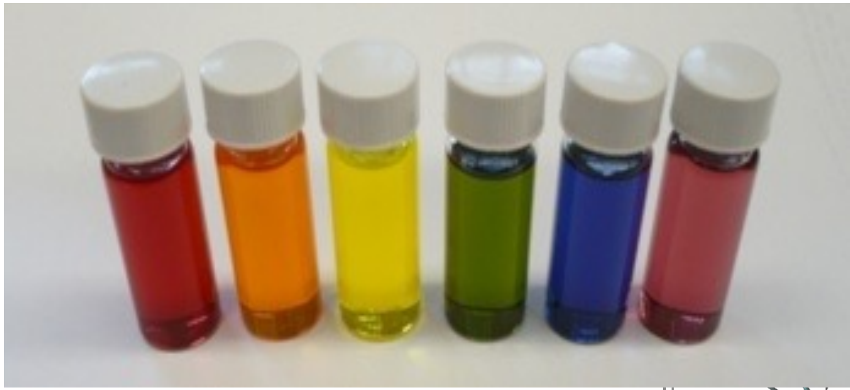

Why does extending the core lead to red shifts?

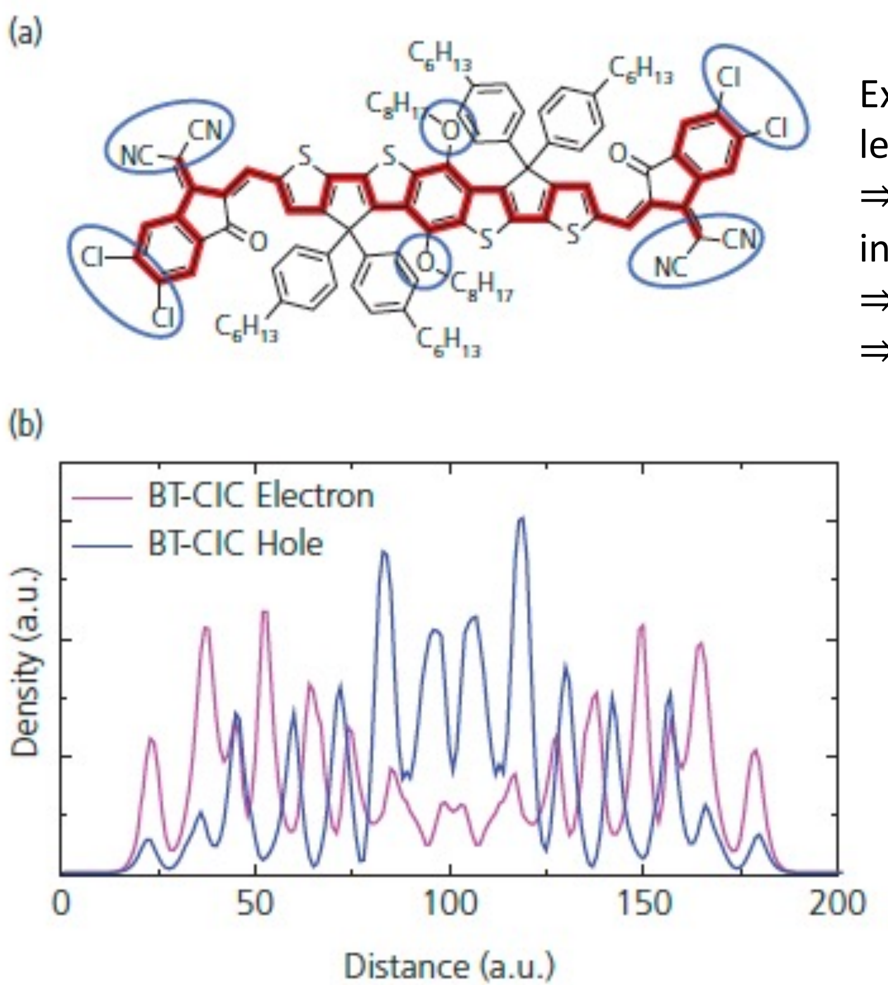

DFT calculation of electron and hole distributions along backbone

Extending the core increases the electron conjugation length (red line)
⇒separation between electron and hole distributions increases
⇒reduced binding energy
⇒reduced energy loss

$$E_{loss} = E_X - qV_{OC}$$

Organic Electronics
Stephen R. Forrest

Liu, et al. Phys. Rev. Applied, 11, 024060 (2019)

Binding energy of exciton a function of molecular "volume"

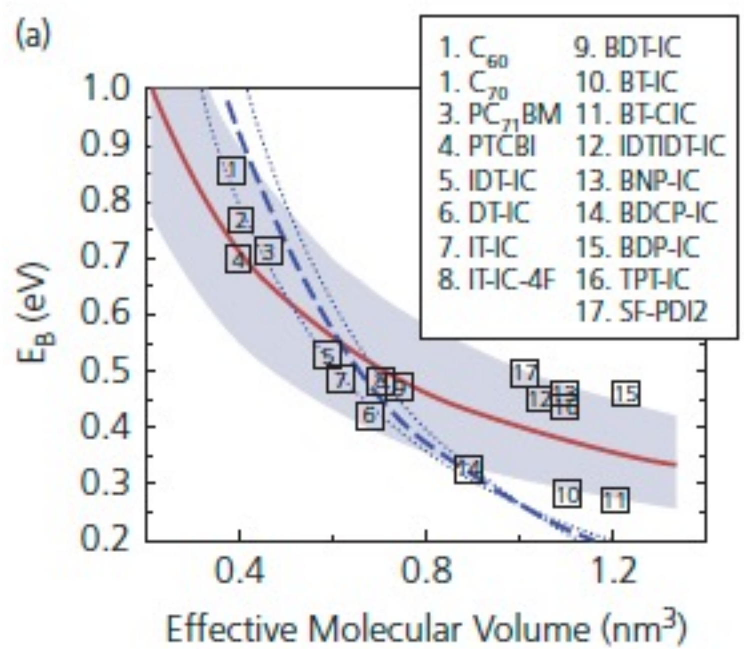

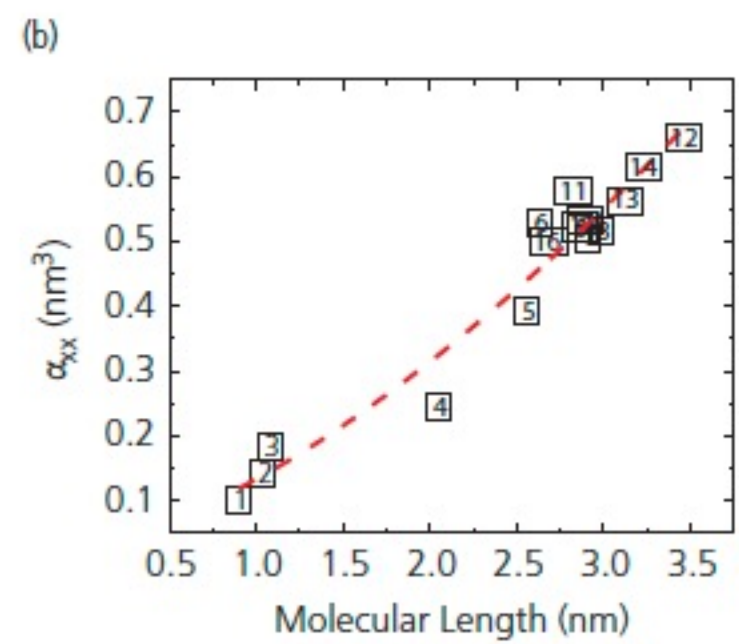

$$E_B = q^2 \int \frac{\left|\Psi_{0,0,0}(\mathbf{r}_h)\right|^2 \left|\Psi_{1,0,0}(\mathbf{r}_e)\right|^2}{4\pi\varepsilon_0 f \left|\mathbf{r}_h - \mathbf{r}_e\right|} d^3\mathbf{r}_h d^3\mathbf{r}_e$$

A single value of dielectric constant (f) fits all molecules (solid line)

$$\alpha_{xx} = \alpha_0 + \alpha_1 l^n$$

Molecular polarizability (related to f) follows same trend with molecular length

Liu, et al. Phys. Rev. Applied, 11, 024060 (2019)

Wavelength-selective Absorption Can Lead to Semitransparent OPVs

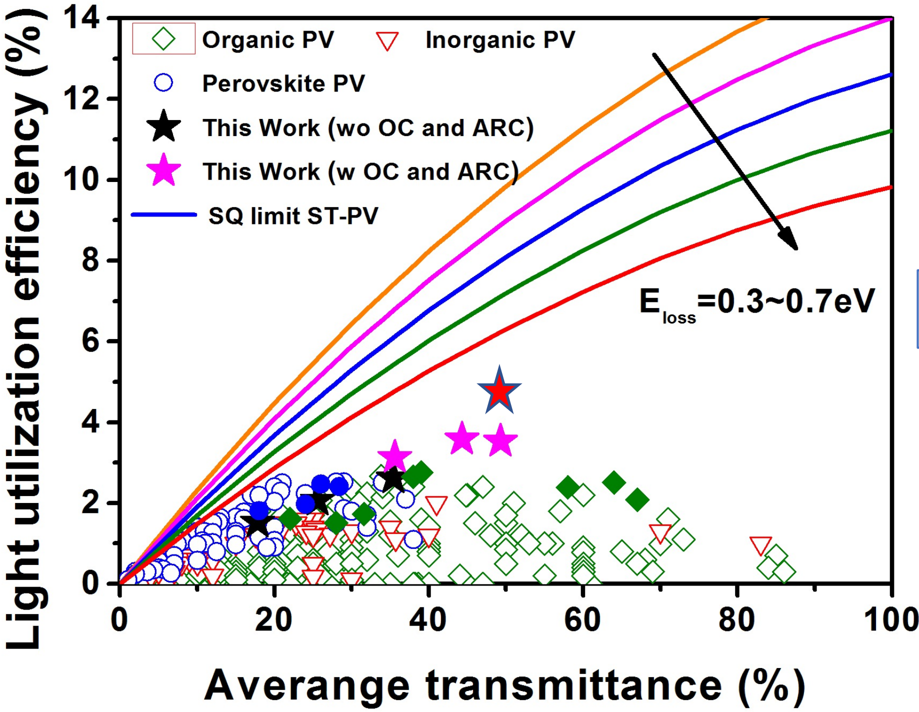

Power generating windows (transparent in the visible, absorbing in the NIR) are a major opportunity unique to OPVs

Transparent OPV Figure of Merit

$$LUE = PCE \times APT$$

LUE: light utilization efficiency
PCE: power conversion efficiency
APT: average photopic transmission

$$\boldsymbol{APT} = \frac{\int T(\lambda)P(\lambda)S(\lambda)d(\lambda)}{\int P(\lambda)S(\lambda)\,d(\lambda)}$$

λ: wavelength; T: transmission
P: photopic response; S: solar photon flux (AM1.5G)

Semi-Transparent Device Materials & Structures

Example of Photon Management

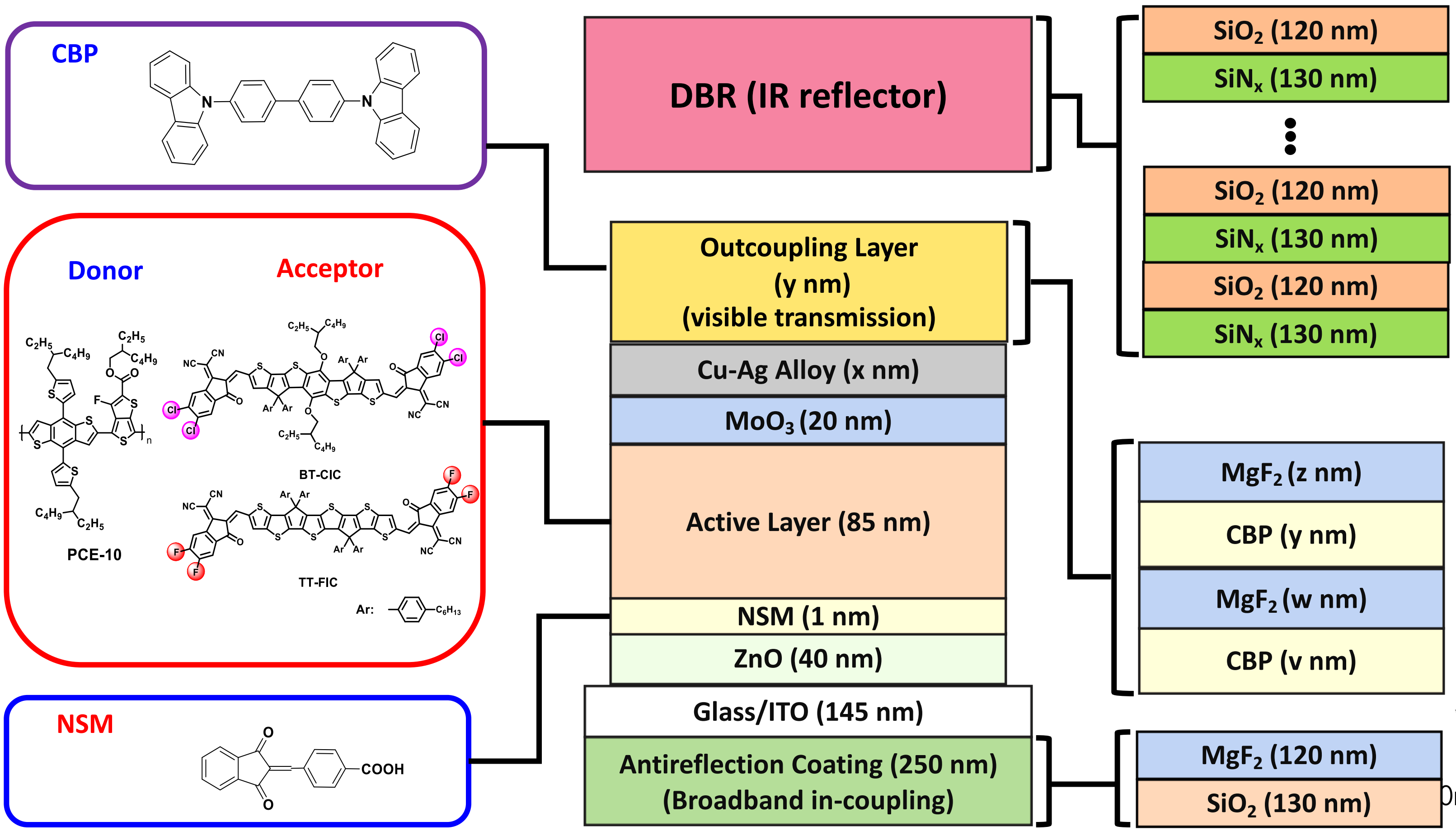

Li, et al. Adv. Mater., 31, 1903173 (2019)

Semi-Transparent Organic Solar Cells

Color Tunable Windows

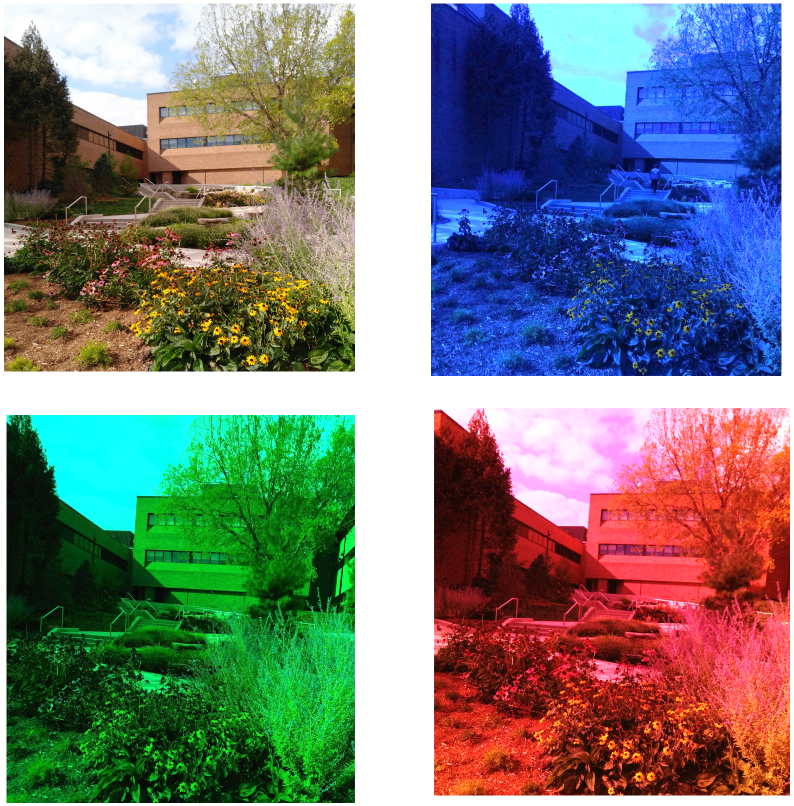

Preferred windows are neutral density

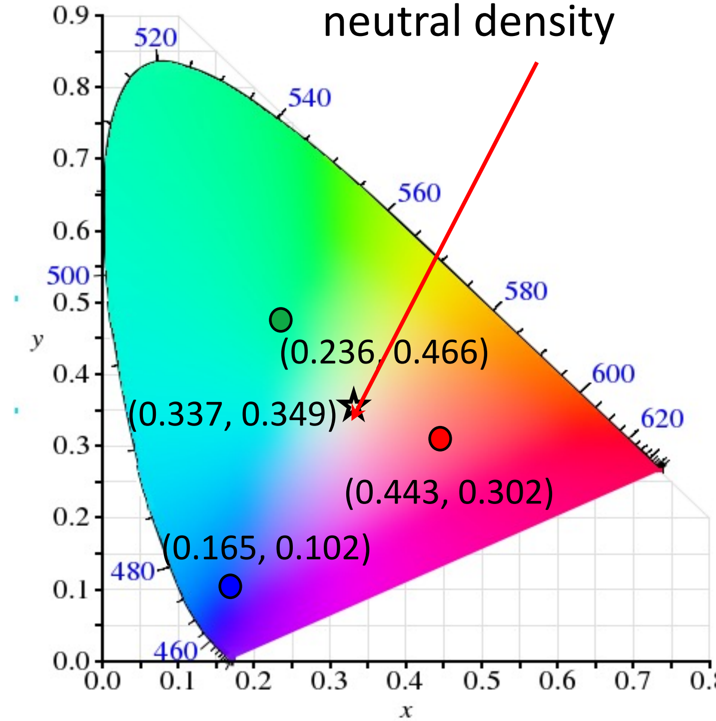

Active Layer	J_{sc} [mA/cm^2]	V_{oc} [V]	FF [%]	PCE [%]
PCE-10:BT-CIC (1:1.5)	**22.5 (21.3)**	**0.70**	**71.0**	**11.2**
PCE-10:DTD-FIC (1:1.5)	**25.6 (21.3)**	**0.64**	**69.5**	**11.3**

Li, et al. Adv. Mater., 31, 1903173 (2019)

Optical Outcoupling Layers

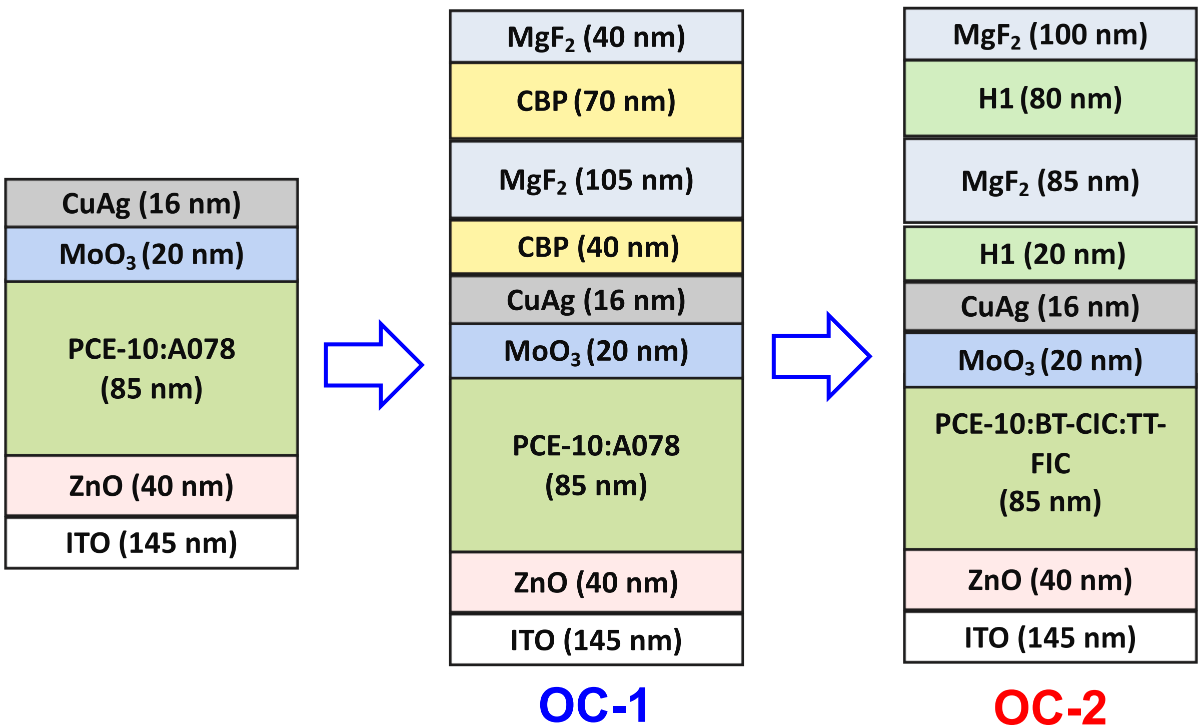

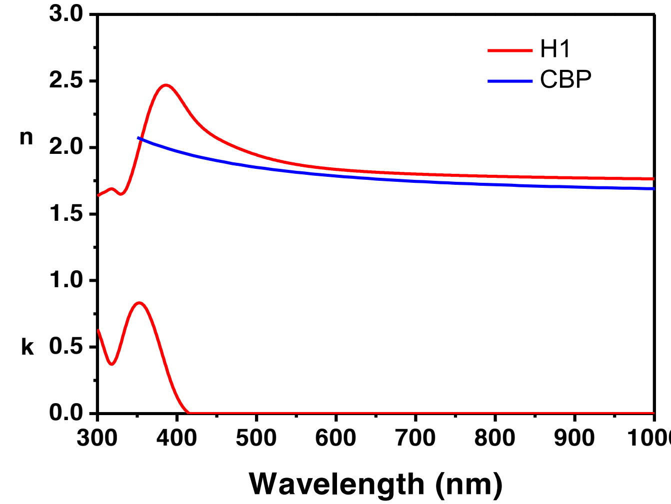

Device	J_{sc} [mA/cm^2]	V_{oc} [V]	FF	PCE [%]	APT [%]	LUE [%]
WO OC	18.4	0.72	0.62	8.3	30.2	2.51
W OC-1	18.1	0.74	0.65	8.7	48.3	4.20
W-OC-2	-	-	-	-	51.2	5.2

Li, et al. Adv. Mater., 31, 1903173 (2019)